



## Chipless-RFID Sensors for Motion Control Applications

Ferran Paredes, Cristian Herrojo, and Ferran Martín

CIMITEC, Departament d'Enginyeria Electrònica, Universitat Autònoma de Barcelona, 08193 Bellaterra, Spain

### Abstract

This paper presents a sensor for the measurement of linear motion, including displacement, velocity and acceleration. For that purpose, a linear chain of metallic inclusions printed or etched at periodic positions on a dielectric substrate is considered. The measurement of displacements and velocities is based on the detection of the inclusions through microwaves when the linear chain of inclusions is in relative motion to the (static) reader, a transmission line based structure fed by a pair of harmonic signals. The inclusions are detected through their effect on the amplitude of the injected signals at the output port of the reader line (giving rise to pulses in the envelope function of the AM modulated signals). As compared to other previous linear displacement and velocity sensors based on a similar approach, in the proposed system the linear chain of inclusions is equipped with an identification (ID) code, where the binary state associated to each inclusion is given by its size. Thus, these electromagnetic encoders are useful for the determination of the chain position by reading a certain (predefined) number of bits, rather than from the cumulative number of pulses (the usual approach). A prototype device is presented in order to validate the approach.

### 1 Introduction

Optical encoders are well-known devices able to precisely provide the angular position, velocity and acceleration of rotor systems, including reactions wheels, servomechanisms, elevator pulleys, etc. [1-3]. Despite the fact that optical encoders exhibit very competitive performance (e.g., spatial resolution), their cost might be prohibitive in certain applications. Moreover, the robustness of optical systems in hostile environments (e.g., with the presence of pollution, dirtiness, or grease, among others) is limited, and this may jeopardize their correct functionality in certain scenarios.

An interesting alternative to optical systems for the measurement of spatial variables are the so-called electromagnetic encoders [4-6]. In these encoders, typically (although not exclusively), metallic inclusions (rather than apertures) are used for the generation of pulses, when the moving element of the sensor is in relative motion to the reader. In an electromagnetic rotary encoder, the metallic inclusions are etched or printed in the periphery of a dielectric disc, the rotor, forming a

circular chain. The static part (called stator in rotary encoder systems) contains the reader, i.e., an element able to detect the presence of inclusions through microwaves, by near-field coupling. Such element is a transmission line based structure fed by a harmonic (interrogation) signal.

The working principle of electromagnetic encoders is conceptually similar to the working principle of optical encoders. Namely, by displacing the chain of inclusions over the transmission line (the sensitive part of the reader), the inclusions modify the transmission coefficient of the line, in particular at the frequency of the harmonic interrogation signal. Consequently, the injected signal is amplitude modulated (AM) at the output port of the reader line, and as many pulses in the envelope function as inclusions in the encoder chain are generated. Thus, knowing the distance between adjacent pulses, the velocity (linear or angular), as well as the acceleration, can be easily inferred. The total displacement with regard to a reference can be inferred from the cumulative number of pulses. However, this incremental-type measurement of encoder position may not be acceptable in certain applications. In this paper, we provide a solution to this problem, by providing an identification (ID) code to the encoder chain. For that purpose, each inclusion provides a bit of information, and the binary state is given by the inclusion size, which alternates between two values. Thus, from the ID code of a certain number of inclusions (a small subset of the whole chain), the absolute position can be inferred.

### 2 The Proposed Reader/Encoder System and Working Principle

The proposed system is inspired by the previous works on electromagnetic rotary encoders [4-6] and near-field chipless-RFID systems [7-18] proposed by the authors. In the rotary encoders reported in [4-6], the main objective was to achieve a high number of pulses per revolution, a figure of merit. Particularly, in [5], 1200 pulses were achieved by considering 600 identical inclusions (split ring resonators) distributed in two circular chains. Moreover, it was demonstrated in [5] the possibility to detect the direction of motion (clockwise or counterclockwise) by adding a non-periodic inclusions' chain in the rotor. Since in [4-6] the inclusions were all identical, the determination of the angular position was merely based on cumulative pulse counting (incremental-type measurement).

For the absolute measurement of displacement, it is necessary to provide an ID code to each position, and this can be done by considering inclusions of different size. In the proposed scheme, each inclusion represents a binary state. Consequently, two different distinguishable inclusion's sizes are needed. In order to determine the absolute position, a minimum number of bits,  $N$ , is required. Such number is given by

$$N \geq \log_2 \left( \frac{L}{p} \right) \quad (1)$$

where  $L$  is the length of the encoder's chain and  $p$  is the period (note that  $L/p$  is thus the number of inclusions). For encoder reading, the bits of the chain are read sequentially, bit by bit. Thus, the encoder position is determined by reading the corresponding bit, plus the previous  $N-1$  bits of the chain. This  $N$ -bit sub-code univocally identifies the encoder position. Obviously, in order to avoid that different positions are identified with the same  $N$ -bit sub-code, the whole ID of the chain cannot be arbitrary. It should be chosen following the De Bruijn sequence [19], which guarantees that any  $N$ -bit sub-code unambiguously identifies the total set of different positions of the encoder. For system functionality, a table with the position assigned to the different  $N$ -bit sub-code sequences is necessary. In case of a system reset, it is necessary that the encoder displaces  $N$  positions, i.e., the number needed to read a complete  $N$ -bit sub-sequence, and thus identify the position from the table. Alternatively, in order to solve a reset fail, a memory to record the absolute position of the encoder can be considered.

The encoders are made of chains of rectangular patches of unequal width (Fig. 1), where the wider and narrow patches correspond to the binary states '1' and '0', respectively. The reader must be able to provide information relative to the time interval between two adjacent patches, and to the size of the patch (binary state). For that purpose, a transmission line loaded with a pair of complementary split ring resonators (CSRRs) [20], etched in the ground plane, is considered (Fig. 2). The smaller CSRR is etched inside the larger one, and it is devoted to the determination of the encoder velocity (and acceleration). Such smaller CSRR is sensitive to the effects of the patches regardless of their size (provided the smaller patches are larger than the smaller CSRR). Thus, it is expected that by injecting a harmonic signal tuned to

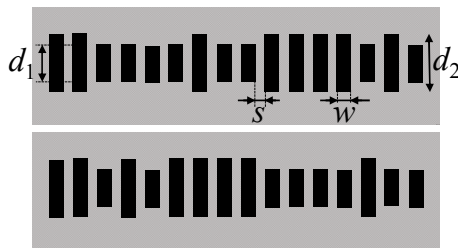


**Figure 1.** Layout of the proposed encoders with unequal patches. Dimensions (in mm) are:  $d_1 = 9.3$ ;  $d_2 = 14.5$ ,  $s = 3$  and  $w = 3$ .

the resonance frequency of such smaller CSRR to the CSRR-loaded line, the instantaneous velocity can be inferred. Each time a patch is on top of the CSRRs, the resonance frequency of the smaller CSRRs will be modified. Therefore, the transmission coefficient at the resonance frequency of the bare CSRR will vary, and a pulse in the envelope function of the amplitude modulated (AM) signal at the output port will appear. Thus, the velocity is given by the time distance between adjacent pulses.

Note, however, that the smaller patches are not expected to substantially modify the resonance frequency of the larger CSRR. This means that if the CSRR-loaded reader line is fed by a harmonic signal tuned to the resonance frequency of the larger CSRR, the peaks in the envelope function at the output port will appear only if a large patch is on top of the CSRRs of the reader line.

According to the previous words, the proposed system needs two combined harmonic signals in order to provide the velocity (and acceleration) and the ID code. For that purpose, a combiner and a diplexer can be implemented, the latter necessary to separately obtain the information relative to the velocity and to the ID code. Alternatively, a switching scheme and a microcontroller can be used, as reported in [21] (see Fig. 3). After the diplexer or switch, an AM detector for each channel is needed, in order to generate the envelope function for each AM signal.

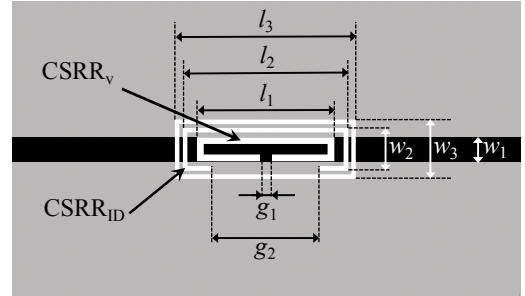


**Figure 2.** Layout of the proposed CSRR-loaded reader line. Dimensions (in mm) are:  $l_1 = 10.3$ ;  $l_2 = 12.3$ ,  $l_3 = 13.5$ ,  $w_1 = 1.9$ ,  $w_2 = 3.1$ ,  $w_3 = 4.3$ ,  $g_1 = 1.0$ ,  $g_2 = 7.2$ . CSRR slots width are  $c_1 = 0.5$  mm and  $c_2 = 0.3$  mm for the inner and the outer CSRR, respectively, and the outer slot ring width is  $c = 0.3$  mm.

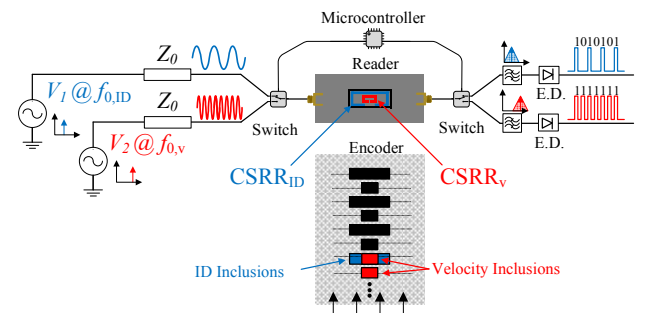


**Figure 3.** Sketch showing the working principle of the proposed reader/encoder system.

### 3 Experimental Validation

To determine the frequencies of both harmonic signals, the response of the bare CSRR-loaded reader line has been measured. The result is depicted in Fig. 4 (the reader line has been fabricated by means of a *LPKF H100* milling machine on the *Rogers RO4003C* substrate with dielectric constant  $\epsilon_r = 3.38$  and thickness  $h = 0.81$  mm). From this figure, the resonance frequencies of the CSRR are found to be  $f_{0,v} = 5.31$  GHz and  $f_{0,ID} = 4.63$  GHz, where the sub-indexes  $v$  (velocity) and ID are used to distinguish both signal frequencies.

For the measurement of the velocity and the determination of the ID code of the chain, the experimental setup shown in Fig. 5 has been utilized. In this paper, rather than using a combiner and a diplexer (or alternatively a microcontroller), we have opted to independently inject the harmonic signals tuned to the above-indicated frequencies. Such signals have been obtained by means of the *Agilent E4438C* signal generator, whereas visualization of the envelope functions has been carried out by means of the *Agilent MSO-X-3104A* oscilloscope. The envelope (AM) detector has been implemented by means of the *Avago HSMS-2860* Schottky diode and the *N2795A* active probe (with capacitance and resistance  $C = 1$  pF and  $R = 1$  M $\Omega$ , respectively). Moreover, a circulator (model *ATM ATc4-8*), acting as an isolator, has been cascaded between the envelope detector and the output port of the reader line, in order to avoid mismatching reflections from the diode. Finally, the linear displacement system model *STM 23Q-3AN* has been used to move the encoder over the reader. Such system provides good accuracy, including the vertical distance between the encoder and the reader (set to 0.5 mm).

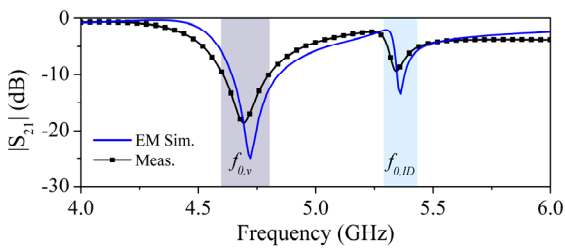


**Figure 4.** Electromagnetic simulation and measured frequency response of the CSRR-loaded reader line.

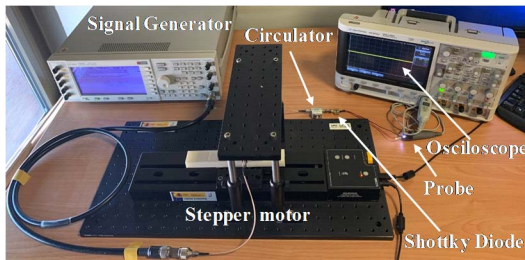


**Figure 5.** Photograph of the experimental setup.

The measured envelope functions corresponding to the encoders depicted in Fig. 1, are shown in Fig. 6 (the encoders have been fabricated in the *Rogers RO4003C* substrate with dielectric constant  $\epsilon_r = 3.38$  and thickness  $h = 0.2$  mm). As it can be appreciated, the envelope function corresponding to the velocity signal, exhibits peaks at periodic positions. The average time between adjacent pulses is 0.6 s, providing a linear velocity of 10 mm/s, i.e., in excellent agreement with the nominal value (10 mm/s). By contrast, for the envelope function associated to the ID code, the peaks only appear when a larger patch is on top of the CSRRs of the reader line. With these results, the validity of the proposed system is demonstrated.

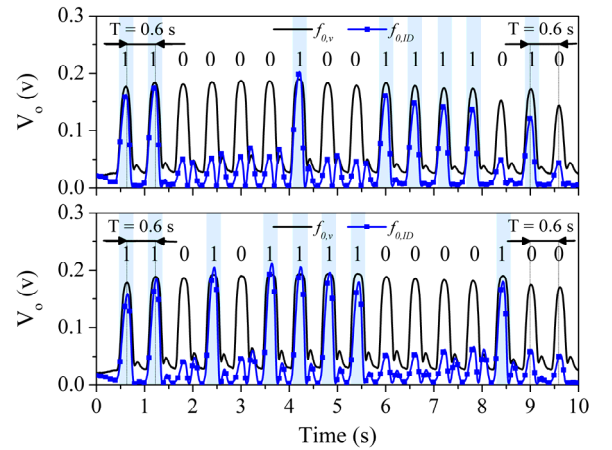


**Figure 6.** Measured envelope functions for the velocity and ID signals.

### 4 Conclusions

In conclusion, an electromagnetic encoder useful for motion control applications has been reported in this paper. The encoder consists of a linear chain of metallic patches etched at periodic positions on a dielectric slab, and the size of the patch determines the binary state associated to it. The reader is a CSRR-loaded line able to detect the presence of a patch (necessary to determine the relative velocity and acceleration of the chain with regard to the reader), and able to discriminate between the larger and smaller patches (consequently providing the ID code of the chain). The main advantage of the proposed system, as compared to previous electromagnetic encoders, is the absolute (rather than incremental-type) determination of the encoder position. The proposed reader is also useful as a near-field chipless-RFID reader with synchronous tag reading, as far as the velocity signal provides the instants of time for bit reading [22].

### 5 Acknowledgements

This work was supported by MICINN-Spain (project TEC2016-75650-R), by Generalitat de Catalunya (project 2017SGR-1159), by Institució Catalana de Recerca i Estudis Avançats (who awarded Ferran Martín), and by FEDER funds.

## 6 References

1. E. Eitel, "Basics of rotary encoders: overview and new technologies", May 2014, *Machine Design Magazine*.
2. G. K. McMillan, D.M. Considine, Eds., *Process Instruments and Controls Handbook*, Fifth Edition, McGraw Hill 1999, ISBN 978-0-07-012582-7, page 5.26.
3. X. Li, J. Qi, Q. Zhang, and Y. Zhang, "Bias-tunable dual-mode ultraviolet photodetectors for photoelectric tachometer," *Appl. Phys. Lett.*, **104**, 4, Jan. 2014, pp. 041108-1–041108-4.
4. J. Mata-Contreras, C. Herrojo, and F. Martín, "Application of split ring resonator (SRR) loaded transmission lines to the design of angular displacement and velocity sensors for space applications", *IEEE Trans. Microw. Theory Techn.*, **65**, 11, Nov. 2017, pp. 4450-4460.
5. Mata-Contreras, C. Herrojo, and F. Martín, "Detecting the rotation direction in contactless angular velocity sensors implemented with rotors loaded with multiple chains of split ring resonators (SRRs)", *IEEE Sensors J.*, **18**, 17, Sep. 2018, pp. 7055-7065.
6. C. Herrojo, J. Mata-Contreras, F. Paredes, and F. Martín, "Microwave encoders for chipless RFID and angular velocity sensors based on S-shaped split ring resonators (S-SRRs)", *IEEE Sensors J.*, **17**, Aug. 2017, pp. 4805-4813.
7. C. Herrojo, J. Mata-Contreras, F. Paredes, Ferran Martín, "Near-field chipless RFID encoders with sequential bit reading and high data capacity", *IEEE MTT-S Int. Microw. Symp. (IMS'17)*, June 2017, Honolulu, Hawaii.
8. C. Herrojo, J. Mata-Contreras, F. Paredes, A. Núñez, E. Ramón, F. Martín, "Near-field chipless-RFID tags with sequential bit reading implemented in plastic substrates", *Int. J. Magnetism. Magnetic Mat.*, **459**, Aug. 2018, pp. 322-327.
9. C. Herrojo, J. Mata-Contreras, F. Paredes, F. Martín, "High data density and capacity in chipless radiofrequency identification (chipless-RFID) tags based on double-chains of S-shaped split ring resonators (S-SRRs)", *EPJ Appl. Metamat.*, **4**, 8, Oct. 2017, 6 pages.
10. C. Herrojo, J. Mata-Contreras, F. Paredes, Ferran Martín, "Near-field chipless RFID system with high data capacity for security and authentication applications", *IEEE Trans. Microw. Theory Techn.*, **65**, 12, Dec. 2017, pp. 5298-5308.
11. C. Herrojo, J. Mata-Contreras, F. Paredes, A. Núñez, E. Ramon, and F. Martín "Near-field chipless-RFID system with erasable/programmable 40-bit tags inkjet printed on paper substrates", *IEEE Microw. Wireless Compon. Lett.*, **28**, Mar. 2018, pp. 272- 274.
12. C. Herrojo, J. Mata-Contreras, F. Paredes, A. Núñez, E. Ramon, and F. Martín, "Very Low-Cost 80-Bit Chipless-RFID Tags Inkjet Printed on Ordinary Paper," *Technologies*, **6**, 2, May 2018, p. 52.
13. C. Herrojo, F. Paredes, J. Mata-Contreras, E. Ramon, A. Núñez, F. Martín, "Time-domain signature barcodes: near-field chipless-RFID systems with high data capacity", *IEEE Microwave Magazine*, **20**, 12, Dec 2019, pp. 87-101.
14. J. Havlicek, C. Herrojo, F. Paredes, J. Mata-Contreras and F. Martín, "Enhancing the per-unit-length data density in near-field chipless-RFID systems with sequential bit reading", *IEEE Ant. Wireless Propag. Lett.*, **18**, 1, Jan. 2019, pp. 89-92.
15. C. Herrojo, F. Muela, J. Mata-Contreras, F. Paredes, F. Martín, "High-density microwave encoders for motion control and near-field chipless-RFID", *IEEE Sensors J.*, **19**, May 2019, pp. 3673-3682.
16. C. Herrojo, F. Paredes, and F. Martín, "Double-stub loaded microstrip line reader for very high data density microwave encoders", *IEEE Trans. Microw. Theory Techn.*, **67**, 9, Sep. 2019, pp. 3527-3536.
17. F. Martín, C. Herrojo, J. Mata-Contreras and F. Paredes, *Time Domain Signature Barcodes for Chipless-RFID and Sensing Applications*, Springer, 2020, Heidelberg.
18. C. Herrojo, F. Paredes, and F. Martín, "3D-printed high data-density electromagnetic encoders based on permittivity contrast for motion control and chipless-RFID", *IEEE Transactions on Microwave Theory and Techniques*, Jan 2020, 10.1109/TMTT.2019.2963176.
19. N.C. de Bruijn, "Acknowledgement of Priority to C. Flye Sainte-Marie on the counting of circular arrangements of  $2n$  zeros and ones that show each  $n$ -letter word exactly once", *T.H.-Report 75-WSK-06*, 1975 Technological University Eindhoven.
20. F. Falcone, T. Lopetegui, J.D. Baena, R. Marqués, F. Martín, and M. Sorolla, "Effective negative- $\epsilon$  stop-band microstrip lines based on complementary split ring resonators", *IEEE Microw. Wireless Compon. Lett.*, **14**, Jun. 2004, pp. 280-282.
21. F. Paredes, C. Herrojo, J. Mata-Contreras, and F. Martín, "Near-field chipless-RFID sensing and identification system with switching reading", *Sensors*, **18**, Apr. 2018, p. 1148.
22. F. Paredes, C. Herrojo, F. Martín, "An approach for synchronous reading of near-field chipless-RFID tags", *10th IEEE International Conference on RFID Technology and Applications (IEEE RFID-TA 2019)*, Sep. 2019, Pisa, Italy.